UCLA
COMPUTATIONAL AND APPLIED MATHEMATICS

Formation of Delta-Shocks and Vacuum States in The Vanishing Pressure Limit of Solutions to the Isentropic Euler Equations

Gui-Qiang Chen
Hailiang Liu

December 2001

CAM Report 01-34

Department of Mathematics
University of California, Los Angeles
Los Angeles, CA. 90095-1555

http://www.math.ucla.edu/applied/cam/index.html

FORMATION OF DELTA-SHOCKS AND VACUUM STATES IN THE VANISHING PRESSURE LIMIT OF SOLUTIONS TO THE ISENTROPIC EULER EQUATIONS

GUI-QIANG CHEN HAILIANG LIU

ABSTRACT. The phenomena of concentration and cavitation and the formation of δ-shocks and vacuum states in the vanishing pressure limit are identified and analyzed in inviscid compressible fluid flow. It is shown that any two-shock Riemann solution of the Euler equations for isentropic fluids tends to a δ-shock solution of the Euler equations for pressureless fluids, and the intermediate density between the two shocks tends to a δ-mass that forms the δ-shock; by contrast, any two-rarefaction-wave Riemann solution for isentropic fluids tends to a two-contact-discontinuity solution for pressureless fluids, and the intermediate state between the two rarefaction waves, even away from the vacuum, tends to a vacuum state. Some numerical results, which exhibit the formation process of δ-shocks and vacuum states, are presented.

1. INTRODUCTION

We are concerned with the phenomena of concentration and cavitation and the formation of δ-shocks and vacuum states in the vanishing pressure limit in inviscid compressible fluid flow. In this paper, we consider the Euler equations of isentropic gas dynamics in the Eulerian coordinates:

$$\partial_t \rho + \partial_x(\rho v) = 0, \tag{1.1}$$

$$\partial_t(\rho v) + \partial_x(\rho v^2 + p) = 0, \tag{1.2}$$

where ρ represents the density, p the scalar pressure, and $m = \rho v$ the momentum, respectively; and ρ and m are in the physical region $\{(\rho, m) \mid \rho \geq 0, |m| \leq V_0 \rho\}$ for some $V_0 > 0$. For $\rho > 0$, $v = m/\rho$ is the velocity with $|v| \leq V_0$. The scalar pressure p is a function of density ρ and a small parameter $\epsilon > 0$ satisfying

$$\lim_{\epsilon \to 0} p(\rho, \epsilon) = 0.$$

For concreteness, we focus on the prototypical pressure function for polytropic gases:

$$p(\rho, \epsilon) = \epsilon p_0(\rho), \qquad p_0(\rho) = \rho^\gamma/\gamma, \quad \gamma > 1. \tag{1.3}$$

Date: December 8, 2001.

1991 *Mathematics Subject Classification.* Primary: 35L65, 35B30, 76E19, 35Q35, 35L67; Secondary: 35B25,65M06.

Key words and phrases. Concentration, cavitation, δ-shocks, vacuum states, Euler equations, vanishing pressure limit, transport equations, measure solutions, isentropic fluids, pressureless fluids, numerical simulations.

System (1.1)–(1.3) is an archetype of hyperbolic systems of conservation laws with form

$$\partial_t u + \partial_x f(u, \epsilon) = 0, \tag{1.4}$$

with $u := (\rho, \rho v)$ and $f(u, \epsilon) := (\rho v, \rho v^2 + p(\rho, \epsilon))$.

In Chang-Chen-Yang [4, 5], a phenomenon of concentration of solutions of the two-dimensional Riemann problem, called a smoothed δ-shock wave, was first observed numerically for the Euler equations of gas dynamics, when Riemann data produce four initial contact discontinuities of different signs and the initial pressure data are close to zero. One of the main objectives of this paper is to show rigorously that the phenomenon of concentration of solutions, observed numerically in [4, 5], in inviscid compressible flow is fundamental, which occurs not only in the multidimensional situations, but also even in the one-dimensional case naturally.

The limit system as $\epsilon \to 0$ formally reduces to the following transport equations:

$$\partial_t \rho + \partial_x(\rho v) = 0, \tag{1.5}$$

$$\partial_t(\rho v) + \partial_x(\rho v^2) = 0, \tag{1.6}$$

which is also called the one-dimensional system of pressureless Euler equations.

The transport equations (1.5) and (1.6) have been analyzed extensively since 1995; for example, see Bouchut-James [1], Bouchut-Jin-Li [2], Brenier-Grenier [3], Grenier [10], E-Rykov-Sinai [9], Huang-Wang [11], Li-Yang [15], Li-Zhang [16, 17], Poupaud-Rascle [18], Sheng-Zhang [24], Wang-Huang-Ding [26], and the references cited therein. Also see Joseph [12], Keyfitz-Kranzer [13], Korchinski [14], Sever [19], Tan-Zhang [22], and Tan-Zhang-Zheng [23] for related equations and results. It has been shown that, for the transport equations, the δ-shocks and vacuum states do occur in the Riemann solutions. Since the two eigenvalues of the transport equations (1.5)-(1.6) coincide, the occurrence of δ-shocks and vacuum states can be regarded as a result of resonance between the two characteristic fields.

In this paper, we rigorously analyze the phenomena of concentration and cavitation and the formation of δ-shocks and vacuum states in the vanishing pressure limit in inviscid, isentropic compressible fluid flow. This limit can be regarded as a singular flux-function limit of entropy solutions of hyperbolic conservation laws (1.4). We show that such phenomena do occur even in the one-dimensional case: any two-shock Riemann solution of the Euler equations for isentropic fluids tends to a δ-shock solution of the Euler equations for pressureless fluids, and the intermediate density between the two shocks tends to a weighted δ-measure that forms a δ-shock; by contrast, any two-rarefaction-wave Riemann solution for isentropic fluids tends to a two-contact-discontinuity solution for pressureless fluids, and the intermediate state between the two rarefaction waves, even away from the vacuum, tends to a vacuum state. This shows that the δ-shocks for the transport equations are a concentration of density, while the vacuum states are a cavitation in the vanishing pressure limit; both are fundamental and physical in fluid dynamics.

From the point of view of hyperbolic conservation laws, since the limiting system is nonstrictly hyperbolic, the phenomena of concentration and cavitation in the vanishing pressure limit can be regarded as a process of resonance formation between the two characteristic fields. These phenomena show that the flux-function limit can be very singular; the spaces of functions, BV or L^∞, may not be well-posed in this limit; and the space of Radon measures, for which the divergences of certain entropy and entropy flux fields are Radon measures, is a natural space in order to deal with the limit in general. In this regard, a theory of divergence-measure fields has been established in Chen-Frid [6, 7].

The organization of this paper is the following. In Section 2, we discuss δ-shocks and vacuum states for the transport equations (1.5) and (1.6) and examine the dependence on the parameter $\epsilon > 0$ of the Riemann solutions for the Euler equations (1.1)–(1.3) for isentropic fluids. In Section 3, we analyze the formation of δ-shocks in the Riemann solutions of the Euler equations (1.1)–(1.3) in the vanishing pressure limit. In Section 4, we analyze the formation of vacuum states in the Riemann solutions, even away from the vacuum, in the vanishing pressure limit for (1.1)–(1.3). In Section 5, we present some representative numerical results, produced by using the higher order ENO scheme designed in [20, 21], to examine the formation process of δ-shocks and vacuum states in the vanishing pressure limit of the Riemann solutions of (1.1)–(1.3).

The main observations and results in this paper were reported in detail by the first author at the International Conference on Nonlinear Evolutionary Partial Differential Equations, Academia Sinica (China), June 10–15, 2001, and at the first Joint Meeting of the American Mathematical Society and the Societe Mathematique de France at ENS de Lyon, France, July 17–20, 2001.

2. Delta-Shocks, Vacuum States, and Riemann Solutions

In this section, we first discuss δ-shocks and vacuum states in the Riemann solutions of the transport equations (1.5) and (1.6), and then we examine the dependence on the parameter $\epsilon > 0$ of the Riemann solutions of the Euler equations of gas dynamics (1.1)–(1.3).

2.1. δ-Shocks and Vacuum States for the Transport Equations. Consider the Riemann problem for the transport equations (1.5) and (1.6) with Riemann initial data

$$(\rho, v)(x, 0) = (\rho_\pm, v_\pm), \qquad \pm x > 0, \tag{2.1}$$

with $\rho_\pm > 0$. Since the equations and the Riemann data are invariant under uniform stretching of coordinates:

$$(x, t) \to (\alpha x, \alpha t),$$

we consider the self-similar solutions of (1.5), (1.6), and (2.1):

$$(\rho, v)(x, t) = (\rho, v)(\xi), \quad \xi = x/t,$$

for which the Riemann problem is reduced to the boundary value problem of the ordinary differential equations:

$$\begin{aligned} &-\xi\rho_\xi + (\rho v)_\xi = 0, \\ &-\xi(\rho v)_\xi + (\rho v^2)_\xi = 0, \\ &(\rho, v)(\pm\infty) = (\rho_\pm, v_\pm). \end{aligned}$$

As shown in [24], in the case $v_- < v_+$, we can obtain a solution which consists of two contact discontinuities and a vacuum state determined by the Riemann data $(\rho_\pm, v_\pm)$. That is,

$$(\rho, v)(\xi) = \begin{cases} (\rho_-, v_-), & -\infty < \xi \le v_-, \\ (0, \xi), & v_- \le \xi \le v_+, \\ (\rho_+, v_+), & v_+ \le \xi < \infty. \end{cases}$$

In the case $v_- > v_+$, a key observation in [24] is that the singularity is impossible to be a jump with finite amplitude, that is, there is no solution which is piecewise smooth and bounded; hence the solutions containing weighted δ-measures supported on curves were constructed as distributional solutions in order to establish the existence from the mathematical point of views (also see [22, 23]).

To define the distributional solutions, the weighted δ-measure $w(t)\delta_S$ supported on a smooth curve S parametrized as $(x(s), t(s))$, $a < s < b$, is defined by

$$(w(\cdot)\delta_S, \psi(\cdot,\cdot)) = \int_a^b w(t(s))\psi(x(s), t(s))\sqrt{x'(s)^2 + t'(s)^2}ds$$

for all $\psi \in C_0^\infty(\mathbb{R}_+^2)$.

With this definition, one can construct a family of solutions for the case $v_- > v_+$. A δ-distributional solution with a parameter σ can be obtained as

$$\rho(x,t) = \rho_0(x,t) + w(t)\delta_S, \qquad v(x,t) = v_- + [v]\,\chi(x - \sigma t),$$

where

$$\rho_0(x,t) = \rho_- + [\rho]\,\chi(x - \sigma t), \qquad w(t) = \frac{t}{1+\sigma^2}(\sigma[\rho] - [\rho v]),$$

with

$$S = \{(x,t) : x = \sigma t,\ 0 \le t < \infty\},$$

$[\omega] := \omega_+ - \omega_-$ denoting the jump of the function ω across the discontinuity, and $\chi(x)$ is the characteristic (or indication) function that is zero when $x < 0$ and is 1 when $x > 0$.

It is shown in [24] that the above δ-distributional solution (ρ, v) satisfies

$$(\rho, \phi_t) + (\rho v, \phi_x) = 0, \tag{2.2}$$

$$(\rho v, \phi_t) + (\rho v^2, \phi_x) = 0, \tag{2.3}$$

for any $\phi \in C_0^\infty(\mathbb{R} \times \mathbb{R}^+)$, where

$$(\rho, \phi) = \int_0^\infty \int_{\mathbb{R}} \phi\rho_0 dxdt + (w(t)\delta_S, \phi),$$

and

$$(\rho v, \phi) = \int_0^\infty \int_{\mathbb{R}} \phi v \rho_0 dxdt + (\sigma w(t)\delta_S, \phi).$$

A unique solution can be singled out by the so called mathematical δ-Rankine-Hugoniot condition:

$$\sigma = \frac{\sqrt{\rho_+}v_+ + \sqrt{\rho_-}v_-}{\sqrt{\rho_+} + \sqrt{\rho_-}},$$

and the $\delta-$entropy condition:

$$\lambda_+ < \sigma < \lambda_-.$$

The entropy condition means that, in the (x,t)-plane, the characteristic lines on both sides of a δ-shock wave are all incoming, which implies that the δ-shocks are overcompresive shocks.

2.2. **Riemann Solutions for the Isentropic Euler Equations.** The Euler equations (1.1)–(1.3) can be written into:

$$\partial_t \rho + \partial_x(\rho v) = 0, \tag{2.4}$$

$$\partial_t(\rho v) + \partial_x(\rho v^2 + \epsilon p_0(\rho)) = 0. \tag{2.5}$$

The eigenvalues of system (2.4) and (2.5) are

$$\lambda_1 = v - c(\rho, \epsilon), \qquad \lambda_2 = v + c(\rho, \epsilon), \qquad \text{for } \rho > 0,$$

with

$$c(\rho, \epsilon) = \sqrt{\epsilon\, p_0'(\rho)} = \sqrt{\epsilon}\, \rho^\theta, \qquad \theta = \frac{\gamma - 1}{2}.$$

The Riemann invariants are

$$w = v + \frac{\sqrt{\epsilon}}{\theta}\rho^\theta, \qquad z = v - \frac{\sqrt{\epsilon}}{\theta}\rho^\theta.$$

Then the Riemann solutions, which are the functions of $\xi = x/t$, are governed by

$$-\xi \rho_\xi + (\rho v)_\xi = 0, \tag{2.6}$$

$$-\xi(\rho v)_\xi + (\rho v^2 + \epsilon\, p_0(\rho))_\xi = 0, \tag{2.7}$$

$$(\rho, v)(\pm\infty) = (\rho_\pm, v_\pm). \tag{2.8}$$

Shock Curves. The Rankine-Hugoniot condition for discontinuous solutions of (2.4) and (2.5) is

$$-\sigma[\rho] + [\rho v] = 0, \qquad -\sigma[\rho v] + [\rho v^2 + \epsilon\, p_0(\rho)] = 0.$$

The Lax entropy condition is

$$\rho_+ > \rho_- \ \ (1-\text{shock}); \qquad \rho_+ < \rho_- \ \ (2-\text{shock}).$$

Then, given a state $u_- \equiv (\rho_-, m_-) = (\rho_-, \rho_- v_-)$, the shock curves, which are the sets of states that can be connected on the right by a 1-shock or 2-shock, in the phase plane are the following:

1-shock curve $S_1(u_-)$:

$$v - v_- = -\sqrt{\frac{1}{\rho\rho_-}\frac{\epsilon\,(p_0(\rho) - p_0(\rho_-))}{(\rho - \rho_-)}}(\rho - \rho_-), \qquad \rho > \rho_-;$$

2-shock curve $S_2(u_-)$:

$$v - v_- = -\sqrt{\frac{1}{\rho\rho_-}\frac{\epsilon\,(p_0(\rho) - p_0(\rho_-))}{(\rho - \rho_-)}}(\rho - \rho_-), \qquad \rho < \rho_-.$$

Then the shock curves are concave or convex, respectively, with respect to $u_- = (\rho_-, m_-)$ in the $\rho - m$ plane.

We now turn to the study of rarefaction-wave solutions of the system. There are two families of rarefaction waves, corresponding to characteristic families λ_1 and λ_2, respectively.

Rarefaction Wave Curves. A rarefaction wave is a continuous solution of (2.6)–(2.8) of form $(\rho, \rho v)(\xi)$, $\xi = x/t$, satisfying

$$\xi = v \mp \sqrt{\epsilon\, p_0'(\rho)}, \qquad -\xi\rho_\xi + (\rho v)_\xi = 0.$$

Then, give a state $u_- = (\rho_-, \rho_- v_-)$, the rarefaction wave curves, which are the sets of states that can be connected on the right by a 1-rarefaction wave or 2-rarefaction wave, in the phase plane are the following:

1-rarefaction wave curve $R_1(u_-)$:

$$v - v_- = -\int_{\rho_-}^{\rho} \frac{\sqrt{\epsilon p_0'(s)}}{s} ds, \qquad \rho < \rho_-;$$

2-rarefaction wave curve $R_2(u_-)$:

$$v - v_- = \int_{\rho_-}^{\rho} \frac{\sqrt{\epsilon p_0'(s)}}{s} ds, \qquad \rho > \rho_-.$$

The rarefaction wave curves are concave or convex, respectively, in the $\rho - m$ plane.

Given a left state $u_- = (\rho_-, m_-)$, the set of states that can be connected on the right by a shock or a rarefaction wave in the phase plane consists of the 1-shock curve $S_1(u_-)$, the 1-rarefaction curve $R_1(u_-)$, the 2-shock curve $S_2(u_-)$, and the 2-rarefaction curve $R_2(u_-)$. These curves divide the phase plane into four regions $S_2S_1(u_-), S_2R_1(u_-), R_2S_1(u_-)$, and $R_2R_1(u_-)$; every right state of the Riemann data staying in one of them yields a unique global Riemann solution $R(x/t)$, which contains a 1-shock (or 1-rarefaction wave) and/or a 2-shock (or 2-rarefaction wave) satisfying

$$w(R(x/t)) \le w(u_R), \;\; z(R(x/t)) \ge z(u_L), \;\; w(R(x/t)) - z(R(x/t)) \ge 0.$$

For example, when $u_+ \in S_2S_1(u_-)$, $R(x/t)$ contains a 1-shock, a 2-shock, and a nonvacuum intermediate constant state; when $u_+ \in R_2R_1(u_-)$, $R(x/t)$ contains a 1-rarefaction wave, a 2-rarefaction wave, and an intermediate constant state that may be a vacuum state. For more details about the Riemann solutions, see [8].

3. Formation of Delta-Shocks in the Vanishing Pressure Limit

In this section, we study the formation of δ-shocks in the vanishing pressure limit of the Riemann solutions of the Euler equations for isentropic fluids.

3.1. **The case** $u_+ \in S_2S_1(u_-)$, $v_- > v_+, \rho_\pm > 0$. Let $u_\epsilon^* := (\rho_\epsilon^*, \rho_\epsilon^* v_\epsilon^*)$ be the intermediate state in the sense that u_- and u_ϵ^* are connected by a 1-shock S_1 with speed σ_1, and that u_ϵ^* and u_+ are connected by a 2-shock S_2 with speed σ_2. Then $(\rho_\epsilon^*, v_\epsilon^*)$ are determined by

$$v_\epsilon^* - v_- = -\sqrt{\frac{1}{\rho_\epsilon^* \rho_-} \frac{\epsilon\,(p_0(\rho_\epsilon^*) - p_0(\rho_-))}{(\rho_\epsilon^* - \rho_-)}}(\rho_\epsilon^* - \rho_-), \qquad \rho_\epsilon^* > \rho_-,$$

and

$$v_+ - v_\epsilon^* = -\sqrt{\frac{1}{\rho_\epsilon^* \rho_+} \frac{\epsilon\,(p_0(\rho_+) - p_0(\rho_\epsilon^*))}{(\rho_+ - \rho_\epsilon^*)}}(\rho_+ - \rho_\epsilon^*), \qquad \rho_\epsilon^* > \rho_+.$$

We have

Lemma 3.1. *For small $\epsilon > 0$, there exists $C > 0$ such that*

$$C^{-1}\epsilon^{-1/\gamma} \le \rho_\epsilon^* \le C\epsilon^{-1/\gamma}.$$

Proof. We define a new function $\phi(s,\tau) = \sqrt{(\frac{1}{s}-\frac{1}{\tau})(p_0(\tau)-p_0(s))}$ for $s,\tau > 0$. Thus, a combination of the jump conditions for the 1-shock and the 2-shock gives

$$v_- - v_+ = \sqrt{\epsilon}\,(\phi(\rho_\epsilon^*,\rho_-) + \phi(\rho_\epsilon^*,\rho_+)) > 0.$$

Letting $\epsilon \to 0$, one must have

$$\lim_{\epsilon\to 0} \phi(\rho_\epsilon^*,\rho_\pm) = \infty,$$

which yields $\lim_{\epsilon\to 0}\rho_\epsilon^* = \infty$. The boundedness of $\sqrt{\epsilon}\,\phi(\rho_\epsilon^*,\rho_\pm)$ implies that $\epsilon\, p_0(\rho_\epsilon^*)$, i.e., $\epsilon\,(\rho_\epsilon^*)^\gamma$ is bounded from both the below and the above. This completes the proof.

Lemma 3.2. *There exists $\sigma \in (v_+, v_-)$ such that*

$$\lim_{\epsilon\to 0} v_\epsilon^* = \sigma;$$

$$\lim_{\epsilon\to 0}\sigma_1^\epsilon = \lim_{\epsilon\to 0}\sigma_2^\epsilon = \sigma;$$

$$\lim_{\epsilon\to 0}\ \rho_\epsilon^*(\sigma_2^\epsilon - \sigma_1^\epsilon) = \sigma[\rho] - [\rho v].$$

Proof. Using the Lax entropy condition for the 1-shock and the 2-shock, we have

$$v_\epsilon^* - \sqrt{\epsilon}\,(\rho_\epsilon^*)^\theta < \sigma_1^\epsilon < v_- - \sqrt{\epsilon}\,(\rho_-)^\theta, \tag{3.1}$$

and

$$v_+ + \sqrt{\epsilon}\,(\rho_+)^\theta < \sigma_2^\epsilon < v_\epsilon^* + \sqrt{\epsilon}\,(\rho_\epsilon^*)^\theta. \tag{3.2}$$

Noting that

$$\sqrt{\epsilon}\,(\rho_\epsilon^*)^\theta = \epsilon^{\frac{1}{2}-\frac{\theta}{\gamma}}(\rho^*\epsilon^{1/\gamma})^\theta = \epsilon^{\frac{1}{2\gamma}}(\rho_\epsilon^*\epsilon^{1/\gamma})^\theta,$$

we see from Lemma 3.1 that, for $\gamma > 1$,

$$\lim_{\epsilon\to 0}\sqrt{\epsilon}\,(\rho_\epsilon^*)^\theta = 0.$$

Letting $\epsilon \to 0$ in (3.1) and (3.2), we have

$$v_+ \le \liminf_{\epsilon\to 0}\ \sigma_2^\epsilon \le \limsup_{\epsilon\to 0}\ \sigma_2^\epsilon \le \liminf_{\epsilon\to 0}\ v_\epsilon^*,$$

and

$$\limsup_{\epsilon\to 0}\ v_\epsilon^* \le \liminf_{\epsilon\to 0}\ \sigma_1^\epsilon \le \limsup_{\epsilon\to 0}\ \sigma_1^\epsilon \le v_-.$$

The Rankine-Hugoniot condition for (2.4) for the 1-shock and the 2-shock implies

$$\rho_\epsilon^*(\sigma_2^\epsilon - \sigma_1^\epsilon) = \sigma_2^\epsilon\,\rho_+ - \sigma_1^\epsilon\,\rho_- - [\rho v],$$

which, together with the fact that $\lim_{\epsilon\to 0}\rho_\epsilon^* = \infty$, gives that

$$\lim_{\epsilon\to 0}\,(\sigma_2^\epsilon - \sigma_1^\epsilon) = 0.$$

This completes the proof of Lemma 3.2.

Lemma 3.3. *The limit σ in Lemma 3.2 is determined by*

$$\sigma = \frac{\sqrt{\rho_+}v_+ + \sqrt{\rho_-}v_-}{\sqrt{\rho_+}+\sqrt{\rho_-}}$$

and satisfies the δ-entropy condition:

$$v_+ < \sigma < v_-.$$

Proof. Using the Rankine-Hugoniot condition for (2.5) for the 1-shock and the 2-shock yields

$$-\sigma_1^\epsilon(\rho_\epsilon^* v_\epsilon^* - \rho_- v_-) + \left(\rho_\epsilon^*(v_\epsilon^*)^2 + \epsilon\, p_0(\rho_\epsilon^*) - \rho_-(v_-)^2 - \epsilon\, p_0(\rho_-)\right) = 0,$$

and

$$-\sigma_2^\epsilon(\rho_\epsilon^* v_\epsilon^* - \rho_+ v_+) + \left(\rho_\epsilon^*(v_\epsilon^*)^2 + \epsilon\, p_0(\rho_\epsilon^*) - \rho_+(v_+)^2 - \epsilon\, p_0(\rho_+)\right) = 0,$$

which give

$$\epsilon\,[p_0(\rho)] + [\rho v^2] + (\sigma_2^\epsilon - \sigma_1^\epsilon)\rho_\epsilon^* v_\epsilon^* + \sigma_1^\epsilon\, \rho_- v_- - \sigma_2^\epsilon\, \rho_+ v_+ = 0.$$

Taking limit $\epsilon \to 0$ and using Lemmas 3.1 and 3.2, we have

$$\sigma^2[\rho] - 2\sigma[\rho v] + [\rho v^2] = 0.$$

When $[\rho] \neq 0$, we have the two roots:

$$\sigma_\pm = \frac{[\rho v] \pm \sqrt{\rho_+ \rho_-}\,[v]}{[\rho]}.$$

Because of

$$v_- > \lim_{\epsilon \to 0} \sigma_j^\epsilon > v_+, \qquad j = 1, 2,$$

we must choose

$$\sigma = \frac{\sqrt{\rho_-}v_- + \sqrt{\rho_+}v_+}{\sqrt{\rho_-} + \sqrt{\rho_+}}.$$

When $[\rho] = 0$, we obtain

$$\sigma = \frac{v_- + v_+}{2}.$$

3.2. **The case $u_+ \in S_2R_1(u_-) \cup R_2S_1(u_-)$, $v_- > v_+, \rho_\pm > 0$.** Since the right state $u_+ = (\rho_+, m_+) \equiv (\rho_+, \rho_+ v_+)$ is fixed and, as ϵ becomes small, the R_1-curve and the S_1-curve become flat, then the right state falls into the region $S_2S_1(u_-)$ when the parameter ϵ is small; and this case is reduced to the case in §3.1, when ϵ is small.

3.3. **Weighted δ-Shocks.** We now show the following theorem characterizing the vanishing pressure limit for the case $v_- > v_+$.

Theorem 3.1. *Suppose that $v_- > v_+$ and $(\rho^\epsilon, m^\epsilon), m^\epsilon = \rho^\epsilon v^\epsilon$, is a two-shock solution of* (2.4) *and* (2.5) *with Riemann data $u_\pm$, constructed in §3.1 and §3.2. Then ρ^ϵ and m^ϵ converge in the sense of distributions, respectively, and the limit functions are the sum of a step function and a δ-measure with weights $\sigma[\rho] - [\rho v]$ and $\sigma[\rho v] - [\rho v^2]$, respectively, which form a δ-shock solution of* (1.5) *and* (1.6) *with the same Riemann data $u_\pm$.*

Proof. 1. Set $\xi = x/t$. Then the Riemann solution can be written as

$$\rho^\epsilon(\xi) = \begin{cases} \rho_-, & \xi < \sigma_1^\epsilon; \\ \rho_\epsilon^*(\xi), & \sigma_1^\epsilon < \xi < \sigma_2^\epsilon; \\ \rho_+, & \xi > s_2^\epsilon, \end{cases}$$

and

$$v^\epsilon(\xi) = \begin{cases} v_-, & \xi < \sigma_1^\epsilon; \\ v_\epsilon^*(\xi), & \sigma_1^\epsilon < \xi < \sigma_2^\epsilon; \\ v_+, & \xi > \sigma_2^\epsilon, \end{cases}$$

satisfying the weak formulation:

$$-\int_{\mathbb{R}}(v^\epsilon-\xi)\rho^\epsilon\,\psi'(\xi)d\xi+\int_{\mathbb{R}}\rho^\epsilon\,\psi(\xi)\,d\xi=0, \tag{3.3}$$

$$-\int_{\mathbb{R}}(v^\epsilon-\xi)\rho^\epsilon v^\epsilon\,\psi'(\xi)d\xi+\int_{\mathbb{R}}\rho^\epsilon v^\epsilon\,\psi(\xi)d\xi=\epsilon\int_{\mathbb{R}}p_0(\rho^\epsilon)\,\psi'(\xi)d\xi, \tag{3.4}$$

for any $\psi\in C_0^1(\mathbb{R})$ satisfying $\psi(\xi)=0$ for $|\xi|\geq R>0$.

2. The first integral in (3.3) can be decomposed, for $\alpha>0$ small, into

$$-\left\{\int_{-R}^{\sigma_1^\epsilon-\alpha}+\int_{\sigma_1^\epsilon-\alpha}^{\sigma_1^\epsilon+\alpha}+\int_{\sigma_1^\epsilon+\alpha}^{\sigma_2^\epsilon-\alpha}+\int_{\sigma_2^\epsilon-\alpha}^{\sigma_2^\epsilon+\alpha}+\int_{\sigma_2^\epsilon+\alpha}^{R}\right\}(v^\epsilon-\xi)\rho^\epsilon(\xi)\psi'(\xi)d\xi, \tag{3.5}$$

in which the second and fourth terms are small, when α is small, since they are bounded by $O(1)\alpha$. The sum of the first and last term of (3.5) is

$$\begin{aligned}
&-\int_{-R}^{\sigma_1^\epsilon-\alpha}(v_--\xi)\rho_-\psi'(\xi)d\xi-\int_{\sigma_2^\epsilon+\alpha}^{R}(v_+-\xi)\rho_+\psi'(\xi)d\xi\\
&=-\rho_-v_-\psi(\sigma_1^\epsilon-\alpha)+\rho_+v_+\psi(\sigma_2^\epsilon+\alpha)+\rho_-(\sigma_1^\epsilon-\alpha)\psi(\sigma_1^\epsilon-\alpha)\\
&\quad-\int_{-R}^{\sigma_1^\epsilon-\alpha}\rho_-\psi(\xi)d\xi-\rho_+(\sigma_2^\epsilon+\alpha)\psi(\sigma_2^\epsilon+\alpha)-\int_{\sigma_2^\epsilon+\alpha}^{R}\rho_+\psi(\xi)d\xi,
\end{aligned}$$

which converges, as $\alpha\to0$ first and then $\epsilon\to0$, to

$$[\rho v]\,\psi(\sigma)-\int_{-R}^{\sigma}\rho_-\,\psi(\xi)d\xi-\int_{\sigma}^{R}\rho_+\,\psi(\xi)d\xi=([\rho v]-\sigma[\rho])\,\psi(\sigma)-\int_{\mathbb{R}}\chi_\rho(\xi-\sigma)\,\psi(\xi)d\xi$$

with

$$\chi_\rho(\xi)=\rho_-+[\rho]\,\chi(\xi),$$

where $\chi(\xi)$ is the characteristic function that is 1 when $\xi>0$ and 0 when $\xi<0$.

3. The third term of (3.5) satisfies

$$\lim_{\epsilon\to0}\lim_{\alpha\to0}\int_{\sigma_1^\epsilon+\alpha}^{\sigma_2^\epsilon-\alpha}(v^\epsilon-\xi)\rho^\epsilon\,\psi'(\xi)d\xi=0. \tag{3.6}$$

This can be seen as follows.

$$\begin{aligned}
&\lim_{\alpha\to0}\int_{\sigma_1^\epsilon+\alpha}^{\sigma_2^\epsilon-\alpha}(v^\epsilon-\xi)\rho^\epsilon\psi'(\xi)d\xi=\int_{\sigma_1^\epsilon}^{\sigma_2^\epsilon}(v_\epsilon^*-\xi)\rho_\epsilon^*\psi'(\xi)d\xi\\
&=\rho_\epsilon^*(\sigma_1^\epsilon-\sigma_2^\epsilon)\left\{-v_\epsilon^*\frac{\psi(\sigma_2^\epsilon)-\psi(\sigma_1^\epsilon)}{\sigma_2^\epsilon-\sigma_1^\epsilon}+\frac{\sigma_1^\epsilon\psi(\sigma_1^\epsilon)-\sigma_2^\epsilon\psi(\sigma_2^\epsilon)}{\sigma_1^\epsilon-\sigma_2^\epsilon}+\frac{1}{\sigma_1^\epsilon-\sigma_2^\epsilon}\int_{\sigma_1^\epsilon}^{\sigma_2^\epsilon}\psi(\xi)d\xi\right\}.
\end{aligned}$$

which, in virtue of the smoothness of the test function $\psi(\xi)$, converges as $\epsilon\to0$ to

$$([\rho v]-\sigma[\rho])\{-\sigma\psi'(\sigma)+\sigma\psi'(\sigma)+\psi(\sigma)-\psi(\sigma)\}=0,$$

where we have used the facts that $\lim_{\epsilon\to0}v_\epsilon^*=\sigma$ and $\lim_{\epsilon\to0}\sigma_j^\epsilon=\sigma$, for $j=1,2$.

On the other hand,

$$-\int_{\mathbb{R}}(v^\epsilon-\xi)\rho^\epsilon\,\psi'(\xi)d\xi+\int\rho^\epsilon\,\psi(\xi)d\xi=0.$$

Then we have

$$\lim_{\epsilon\to0}\int_{\mathbb{R}}(\rho^\epsilon-\chi_\rho(\xi-\sigma))\,\psi(\xi)d\xi=(\sigma[\rho]-[\rho v])\,\psi(\sigma),$$

for any function $\psi \in C_0^\infty(\mathbb{R})$.

3. We now turn to justify the limit of the momentum $m^\epsilon = \rho^\epsilon v^\epsilon$ using the weak formulation of the momentum equation (3.4). As done previously, we can obtain the limit for the first term on the left of (3.4) as

$$-\lim_{\epsilon\to 0}\int_{\mathbb{R}}(v^\epsilon-\xi)\,\rho^\epsilon v^\epsilon\psi'(\xi)d\xi = \psi(\sigma)\,([\rho v^2]-\sigma[\rho v])-\int_{-R}^{\sigma}\rho_- v_-\,\psi(\xi)d\xi-\int_{\sigma}^{R}\rho_+ v_+\,\psi(\xi)d\xi.$$

The term on the right of (3.4), for $\alpha > 0$ small, equals to

$$\epsilon\int_{\mathbb{R}} p_0(\rho^\epsilon)\,\psi'(\xi)d\xi = \epsilon\left\{\int_{-R}^{\sigma_1^\epsilon-\alpha}+\int_{\sigma_1^\epsilon-\alpha}^{\sigma_1^\epsilon+\alpha}+\int_{\sigma_1^\epsilon+\alpha}^{\sigma_2^\epsilon-\alpha}+\int_{\sigma_2^\epsilon-\alpha}^{\sigma_2^\epsilon+\alpha}+\int_{\sigma_2^\epsilon+\alpha}^{R}\right\}p_0(\rho^\epsilon)\,\psi'(\xi)d\xi,$$

which, for $\alpha\to 0$, converges to

$$\begin{aligned}&\epsilon\,\{(p_0(\rho_-)\psi(\sigma_1^\epsilon)+p_0(\rho_\epsilon^*)(\psi(\sigma_2^\epsilon)-\psi(\sigma_1^\epsilon))-p_0(\rho_+)\psi(\sigma_2^\epsilon)\}\\&\quad= o(\epsilon)+\epsilon\,p_0(\rho_\epsilon^*)(\psi(\sigma_2^\epsilon)-\psi(\sigma_1^\epsilon))\to 0,\quad \text{as}\quad \epsilon\to 0,\end{aligned}$$

where we used the fact that $\epsilon p_0(\rho_\epsilon^*)$ is bounded and $\lim_{\epsilon\to 0}\sigma_j^\epsilon=\sigma$, for $j=1,2$.

Returning to the weak formulation, one has

$$\lim_{\epsilon\to 0}\int_{\mathbb{R}}(\rho^\epsilon v^\epsilon-\chi_{\rho v}(\xi-\sigma))\psi(\xi)d\xi=\psi(\sigma)(\sigma[\rho v]-[\rho v^2]),$$

with

$$\chi_{\rho v}(\xi)=\rho_- v_- + [\rho v]\,\chi(\xi).$$

4. Finally, we are in a position to study the limit of ρ^ϵ and m^ϵ by tracking the time-dependence of the weight of the δ-measure in the limit.

Let $\phi(x,t)\in C_0^2(\mathbb{R}\times\mathbb{R}^+)$ be a smooth test function and $\tilde\phi(\xi,t):=\phi(\xi t,t)$. Then we have

$$\lim_{\epsilon\to 0}\int_0^\infty\int_{\mathbb{R}}\rho^\epsilon(x/t)\phi(x,t)dxdt=\lim_{\epsilon\to 0}\int_0^\infty t\left(\int_{\mathbb{R}}\rho^\epsilon(\xi)\tilde\phi(\xi,t)d\xi\right)dt,$$

since ρ^ϵ is a self-similar solution depending only on $\xi = x/t$. Therefore, we have

$$\begin{aligned}\lim_{\epsilon\to 0}\int_{\mathbb{R}}\rho^\epsilon(\xi)\tilde\phi(\xi,t)d\xi&=\int_{\mathbb{R}}\chi_\rho(\xi-\sigma)\tilde\phi(\xi,t)d\xi+(\sigma[\rho]-[\rho v])\tilde\phi(\sigma,t)\\&=t^{-1}\int_{\mathbb{R}}\chi_\rho(x-\sigma t)\phi(x,t)dx+(\sigma[\rho]-[\rho v])\phi(\sigma t,t).\end{aligned}$$

Combining the above two relations, we have

$$\begin{aligned}&\lim_{\epsilon\to 0}\int_0^\infty\int_{\mathbb{R}}\rho^\epsilon(x/t)\phi(x,t)dxdt\\&\quad=\int_0^\infty\int_{\mathbb{R}}\chi_\rho(x-\sigma t)\phi(x,t)dxdt+\int_0^\infty t([\rho v]-\sigma[\rho])\phi(\sigma t,t)dt.\end{aligned}$$

The last term, by definition, equals to

$$< w_1(t)\delta_S,\phi(x,t) >$$

with

$$w_1(t)=\frac{t}{\sqrt{1+\sigma^2}}(\sigma[\rho]-[\rho v]).$$

Similarly, we can show that

$$\begin{aligned}&\lim_{\epsilon\to 0}\int_0^\infty\int_{\mathbb{R}}(\rho^\epsilon v^\epsilon)(x/t)\phi(x,t)dxdt\\ &=\int_0^\infty\int_{\mathbb{R}}\chi_{\rho v}(x-\sigma t)\phi(x,t)dxdt+<w_2(t)\delta_S,\phi(x,t)>\end{aligned}$$

with

$$w_2(t)=\frac{t}{\sqrt{1+\sigma^2}}(\sigma[\rho v]-[\rho v^2]).$$

This completes the proof of Theorem 3.1.

4. Formation of Vacuum States in the Vanishing Pressure Limit

In this section, we show the formation of vacuum states in the vanishing pressure limit of the Riemann solutions of (2.4) and (2.5), even when the Riemann solutions may stay away from the vacuum.

4.1. **The case $u_+ \in R_2R_1(u_-), v_- < v_+, \rho_\pm > 0$.** As recalled previously, for the rarefaction case, the solution is either a constant or satisfies

$$\xi = x/t = v^\epsilon \pm \sqrt{\epsilon\, p_0'(\rho^\epsilon)}. \tag{4.1}$$

More precisely, we have

$$\xi = v^\epsilon - \sqrt{\epsilon\, p_0'(\rho^\epsilon)},$$

for

$$v_- - \sqrt{\epsilon\, p_0'(\rho_-)} < \xi < v_\epsilon^* - \sqrt{\epsilon\, p_0'(\rho_\epsilon^*)};$$

and

$$\xi = v^\epsilon + \sqrt{\epsilon\, p_0'(\rho^\epsilon)},$$

for

$$v_\epsilon^* + \sqrt{\epsilon\, p_0'(\rho_\epsilon^*)} < \xi < v_+ + \sqrt{\epsilon\, p_0'(\rho_+)}.$$

In the phase plane, the right state is in the region $R_2R_1(u_-)$. The point on the R_1-curve satisfies

$$v_\epsilon^* = v_- - \int_{\rho_-}^{\rho_\epsilon^*}\frac{\sqrt{\epsilon\, p_0'(s)}}{s}ds \le v_- + \int_0^{\rho_-}\frac{\sqrt{\epsilon\, p_0'(s)}}{s}ds = v_- + \frac{2\sqrt{\epsilon}}{\gamma-1}\rho_-^{\frac{\gamma-1}{2}} = A.$$

Then it is easy to see that the R_1-curve ends at $(0, A)$. For any point (ρ_+, ρ_+v_+) with $v_+ > A$, it can be connected only with a 2-rarefaction wave on the left by a vacuum state. Then there are two subcases:

Subcase 1: $v_- < v_+ < A$. In this case, there is no vacuum in the solution. The intermediate state $(\rho_\epsilon^*, m_\epsilon^*)$ satisfies

$$m_\epsilon^* = \rho_\epsilon^* v_- - \rho_\epsilon^*\int_{\rho_-}^{\rho_\epsilon^*}\frac{\sqrt{\epsilon\, p_0'(s)}}{s}ds, \qquad \rho_\epsilon^* < \rho_-,$$

and

$$m_+ = \rho_+\frac{m_\epsilon^*}{\rho_\epsilon^*} + \rho_+\int_{\rho_-}^{\rho_\epsilon^*}\frac{\sqrt{\epsilon\, p_0'(s)}}{s}ds, \qquad \rho_+ > \rho_\epsilon^*.$$

Due to the boundedness of the integral term, when $\epsilon \to 0$, we have

$$\lim_{\epsilon\to 0} m_\epsilon^* = v_- \lim_{\epsilon\to 0}\rho_\epsilon^*$$

and

$$m_+ = \rho_+ \lim_{\epsilon\to 0} m_\epsilon^* / \lim_{\epsilon\to 0} \rho_\epsilon^*.$$

One must have $\lim_{\epsilon\to 0}\rho_\epsilon^* = 0$ and $\lim_{\epsilon\to 0} m_\epsilon^* = 0$, since, otherwise $v_+ = v_-$ which is a contradiction with the assumption $v_+ > v_-$.

To figure out the limit of the speed, we let $\epsilon \to 0$ in the relation (4.1), which gives

$$\lim_{\epsilon\to 0} v^\epsilon(\xi) = \xi \mp \lim_{\epsilon\to 0}\sqrt{\epsilon p_0'(\rho^\epsilon)},$$

for $v_- < \xi \le \lim_{\epsilon\to 0}\lambda_1(\rho_\epsilon^*, m_\epsilon^*)$ or $\lim_{\epsilon\to 0}\lambda_2(\rho_\epsilon^*, m_\epsilon^*) \le \xi < v_+$. The uniform boundedness of ρ^ϵ with respect to ϵ leads to

$$\lim_{\epsilon\to 0}(\lambda_2(\rho_\epsilon^*, m_\epsilon^*) - \lambda_1(\rho_\epsilon^*, m_\epsilon^*)) = 0,$$

and hence

$$\lim_{\epsilon\to 0} v^\epsilon(\xi) = \xi, \qquad v_- < \xi < v_+.$$

To summarize, the limit solution for (ρ, v) in this case is

$$(\rho, v)(\xi) = \begin{cases} (\rho_-, v_-), & -\infty < \xi \le v_-, \\ (0, \xi), & v_- \le \xi \le v_+, \\ (\rho_+, v_+), & v_+ \le \xi < \infty. \end{cases}$$

Subcase 2: $v_+ \ge A$. In this case, there is a vacuum state in the Riemann solution itself. The intermediate state $(\rho_\epsilon^*, m_\epsilon^*) = (0, 0)$ is a vacuum state. When passing to the limit, the limit solution coincides with the one in Case 1.

4.2. **Case** $u_+ \in S_2R_1(u_-) \cup R_2S_1(u_-)$, $v_- < v_+, \rho_\pm > 0$. Since the right state $u_+ = (\rho_+, \rho_+v_+)$ is fixed and, as ϵ becomes small, the R_1-curve becomes flat, then the right state falls into the region $R_2R_1(u_-)$ when the parameter ϵ is small; and then this case is reduced to the case in §4.1 when ϵ is small.

5. Formation Process of Delta-Shock and Vacuum States: Numerical Simulations

To see the formation process of δ-shocks and vacuum states in the vanishing pressure limit of the Riemann solutions of the Euler equations (2.4) and (2.5), we present a selected group of representative numerical results. We have performed many more numerical tests to make sure what we present are not numerical artifacts.

To discretize the system, we use the higher order ENO scheme to obtain a method-of-line ODE in time, and then discretize the ODE by the classical higher order explicit Runge-Kutta method, see [20, 21]. We will use the algorithms suggested in [21].

To see the concentrate phenomenon, we solve the Riemann problem for (1.1)–(1.3) with $p = \rho^\gamma/\gamma$ and $\gamma = 1.4$ for an ideal gas. The initial data are

$$(\rho, v)(x, 0) = \begin{cases} (1.0, 1.5), & \text{if } x < 0, \\ (0.2, 0.0), & \text{if } x > 0. \end{cases}$$

We compute by the third-order ENO scheme, [21], up to $t = 0.2$ with mesh 100. The numerical simulations for different choices of ϵ are presented in Figures 5.1-5.6. These figures show the formation process of a δ-shock in the vanishing pressure limit of the two-shock Riemann solutions in isentropic Euler flow. We start with $\epsilon/\gamma = 1.0$ and then $\epsilon/\gamma = 0.50, 0.10, 0.05, 0.01$ decrease up to $\epsilon/\gamma = 0.001$. Figs. 5.1a–5.6a show the concentration of the density yielding a weighted δ-measure in the limit, in which the horizontal axis stands for the space variable x and the vertical axis stands for the density. Figs. 5.1b–5.6b show the change of the velocity as ϵ decreases yielding a step function in the limit, in which the horizontal axis stands for the space variable x and the vertical axis stands for the velocity.

We can see clearly from these numerical results that, when ϵ decreases, the locations of the two shocks become closer, and the density of the intermediate state increases dramatically, while the velocity is closer to a step function; in the vanishing pressure limit, the two shocks coincide to form, along with the intermediate state, a δ-shock of the transport equations (1.5) and (1.6), while the velocity is a step function.

The cavitation phenomenon is simulated for the Riemann problem (1.1)-(1.3) with initial data

$$(\rho, v)(x, 0) = \begin{cases} (1.0, 0), & \text{if} \quad x < 0 \\ (0.2, 1.5), & \text{if} \quad x > 0. \end{cases}$$

In the rarefaction wave cases, we employ the first-order ENO scheme to compute the solution up to $t = 0.2$. Numerical simulations are presented in Figures 5.7-5.12. These figures show the formation process of a vacuum state in the vanishing pressure limit of the two-rarefaction-wave Riemann solutions, starting away from the vacuum, in isentropic Euler flow. We start with $\epsilon/\gamma = 1.0$ and then $\epsilon/\gamma = 0.50, 0.10, 0.05, 0.01$ decrease up to $\epsilon/\gamma = 0.001$. Figs. 5.7a–5.12a show the cavitation of the density yielding a vacuum state between the left boundary of the 1-rarefaction wave and the right boundary of the 2-rarefaction wave in the limit, in which the horizontal axis stands for the space variable x and the vertical axis is stands for the density. Figs. 5.7b–5.12b show the change of the momentum as ϵ decreases yielding a linear function between the left boundary of the 1-rarefaction wave and the right boundary of the 2-rarefaction wave in the limit, in which the horizontal axis stands for the space variable x and the vertical axis stands for the momentum.

We can see clearly from these numerical results that, when ϵ decreases, the left boundary of the 1-rarefaction wave and the right boundary of the 2-rarefaction wave are fixed; the right boundary of the 1-rarefaction wave and the left boundary of the 2-rarefaction wave become closer and closer, while the states between the left boundary of the 1-rarefaction wave and the right boundary of the 2-rarefaction wave in the Riemann solution tends to a vacuum state; and, in the limit, the left boundary of the 1-rarefaction wave and the right boundary of the 2-rarefaction wave become two contact discontinuities of the transport equation (1.5) and (1.6).

Acknowledgments

Gui-Qiang Chen's research was supported in part by the National Science Foundation under Grants DMS-9971793, INT-9987378, and INT-9726215. Hailiang Liu's research was supported in part by the National Science Foundation under Grant DMS-01-07917.

References

[1] F. Bouchut and F. James, Duality solutions for pressureless gases, monotone scalar conservation laws, and uniqueness, *Commun. Partial Diff. Eqs.* **24** (1999), 2173–2189.

[2] F. Bouchut, Shi Jin, and X. Li, Numerical approximation of pressureless and isothermal gas dynamics, Preprint, November 2001.

[3] Y. Brenier and E. Grenier, Sticky particles and scalar conservation laws, *SIAM J. Numer. Anal.* **35** (1998), 2317–2328.

[4] T. Chang, G.-Q. Chen, S. Yang, 2-D Riemann problem in gas dynamics and formation of spiral, In: *Nonlinear Problems in Engineering and Science–Numerical and Analytical Approach (Beijing, 1991)*, pp. 167–179, Science Press: Beijing, 1992.

[5] T. Chang, G.-Q. Chen, S. Yang, On the Riemann problem for two-dimensional Euler equations, I: Interaction of shocks and rarefaction waves, Discrete Contin. Dynam. Systems, **1** (1995), 555–584; II: Interaction of contact discontinuities, Discrete Contin. Dynam. Systems, **6** (2000), 419–430.

[6] G.-Q. Chen and H. Frid, Divergence-measure fields and hyperbolic conservation laws, Arch. Rational Mech. Anal. **147** (1999), 89–118.

[7] G.-Q. Chen and H. Frid, Extended divergence-measure fields and the Euler equations of gas dynamics, Preprint, Northwestern Univeristy, August 2001.

[8] G.-Q. Chen and D. Wang, The Cauchy problem for the Euler equations for compressible fluids, In: *Handbook of Mathematical Fluid Dynamics,* Vol. **1**, Elsevier, 2002.

[9] W. E, Yu. G. Rykov, and Ya. G. Sinai, Generalized variational principles, global weak solutions and behavior with random initial data for systems of conservation laws arising in adhesion particle dynamics, *Commun. Math. Phys.* **177** (1996), 349–380.

[10] E. Grenier, Existence globale pour le système des gaz sans pression, *C. R. Acad. Sci. Paris Sér. I. Math.* **321** (1995), 171–174.

[11] F. Huang and Z. Wang, Well posedness for pressureless flow, *Commun. Math. Phys.* **222** (2001), 117-146.

[12] K. T. Joseph, A Riemann problem whose viscosity solutions contain delta measure, *Asymptotic Analysis,* **7** (1993), 105-120.

[13] B. L. Keyfitz and H. Kranzer, Spaces of weighted measures for conservation laws with singular shock solutions, *J. Diff. Eqs.* **118** (1995), 420–451.

[14] D. J. Korchinski, Solutions of a Riemann problem for a 2×2 system of conservation laws possessing no classical solution, Adelphi University Thesis, 1977.

[15] J. Li and H. Yang, Delta-shocks as limits of vanishing viscosity for multidimensional zero-pressure gas dynamics, *Quart. Appl. Math.* **59** (2001), 315–342.

[16] J. Li and T. Zhang, Generalized Rankine-Hugoniot relations of delta-shocks in solutions of transportation equations, In: *Advances in Nonlinear Partial Differential Equations and Related Areas* (Beijing, 1997), 219–232, eds. G.-Q. Chen et al, World Sci. Publishing: River Edge, NJ, 1998.

[17] J. Li and T. Zhang, On the initial-value problem for zero-pressure gas dynamics, In: *Hyperbolic Problems: Theory, Numerics, Applications*, Vol. **2** (Zürich, 1998), 629–640, Birkhäuser: Basel, 1999.

[18] F. Poupaud and M. Rascle, Measure solutions to the linear multi-dimensional transport equation with non-smooth coefficients, *Commun. Partial Diff. Eqs.* **22** (1997), 337–358.

[19] M. Sever, A class of nonlinear, nonhyperbolic systems of conservation laws with well-posed initial value problem, Preprint, Hebrew University, 2000.

[20] C.W. Shu, S. Osher, Efficient implementation of essentially nonoscillatory shock-capturing schemes, *J. Comput. Phys.* **77** (1988), 439–471.

[21] C.W. Shu, S. Osher, Efficient implementation of essentially nonoscillatory shock-capturing schemes. II., *J. Comput. Phys.* **83** (1989), 32–78.

[22] D. Tan and T. Zhang, Two dimensional Riemann problem for a hyperbolic system of nonlinear conservation laws I: four-J cases, J. Diff. Eqs. **111** (1994), 203-254; II: Initial data involving some rarefaction waves, J. Diff. Eqs. **111** (1994), 255-283.

[23] D. Tan, T. Zhang, and Y. Zheng, Delta-shock waves as limits of vanishing viscosity for hyperbolic system of conservation laws, J. Diff. Eqs. **112** (1994), 1-32.

[24] W. Sheng and T. Zhang, *The Riemann Problem for the Transport Equations in Gas Dynamics*, Mem. Amer. Soc. **654** (1999), AMS: Providence.

[25] Z. Wang and X. Ding, Uniqueness of generalized solutions for the Cauchy problem of transportation equations, *Acta Math. Sci.* (English Ed.), **17** (1997), 341-352.

[26] Z. Wang, F. Huang, and X. Ding, On the Cauchy problem of transportation equations, *Acta Math. Appl. Sinica (English Ser.)*, **13** (1997), 113–122.

[27] Ya. B. Zeldovich, Gravitational instability: an approximate theory for large density perturbations, Astronaut. Astrophys. **5** (1970), 84-89.

Gui-Qiang Chen
Department of Mathematics, Northwestern University
2033 Sheridan Road
Evanston, IL 60208-2730, USA
gqchen@math.northwestern.edu
Homepage: http://www.math.northwestern.edu/~gqchen/preprints

Hailiang Liu
Department of Mathematics, University of California at Los Angeles
Los Angeles, CA 90095-1555, USA
hliu@math.ucla.edu
Homepage: http://www.math.ucla.edu/~hliu

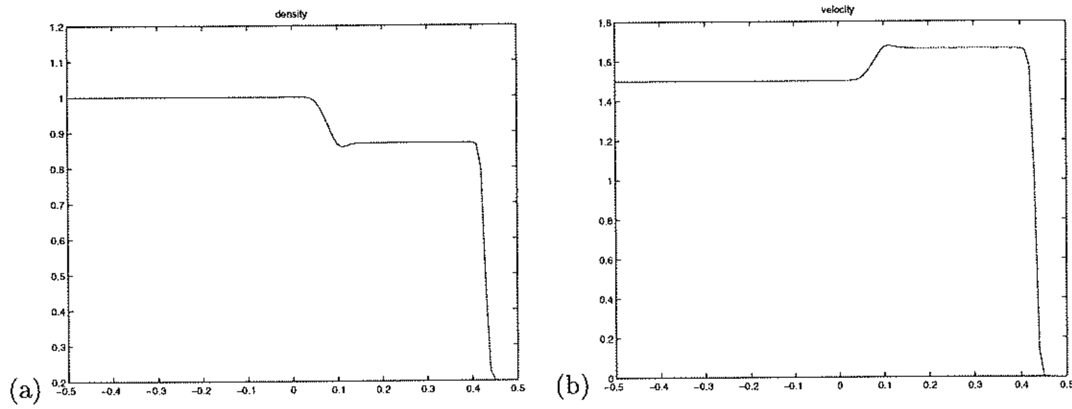

FIGURE 5.1. Density and velocity for $\epsilon = 1.4$

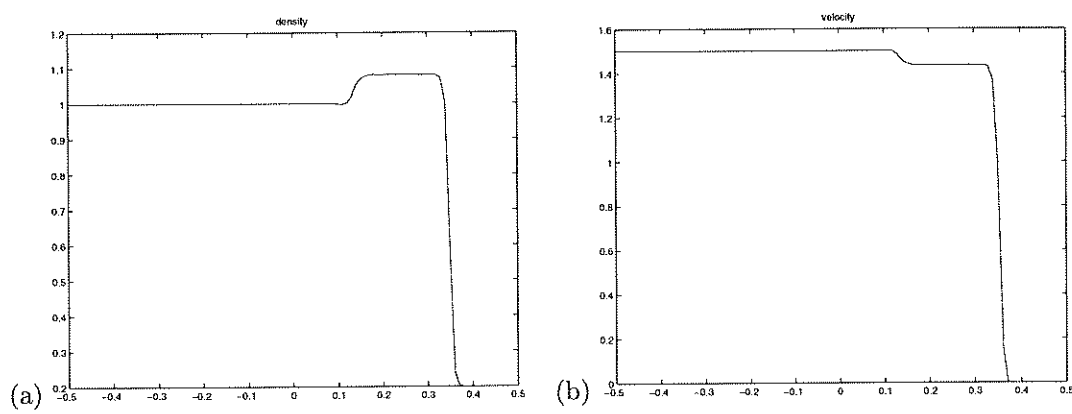

FIGURE 5.2. Density and velocity for $\epsilon = 0.70$

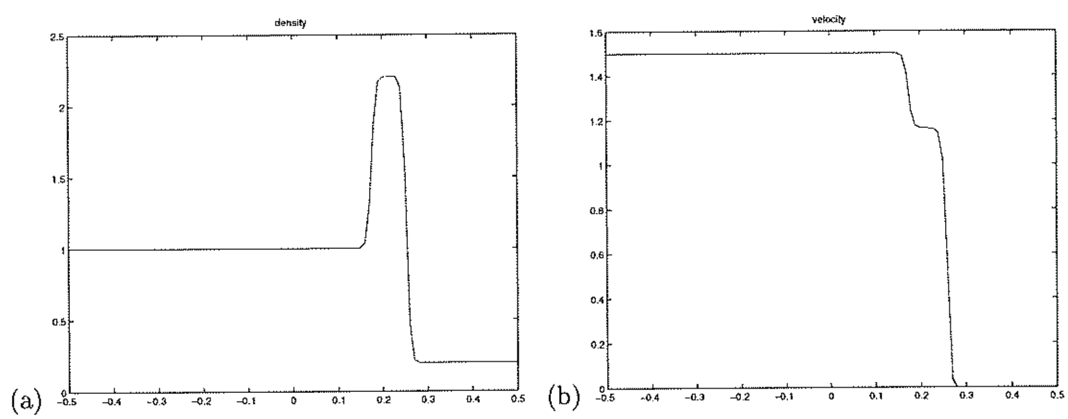

FIGURE 5.3. Density and velocity for $\epsilon = 0.14$

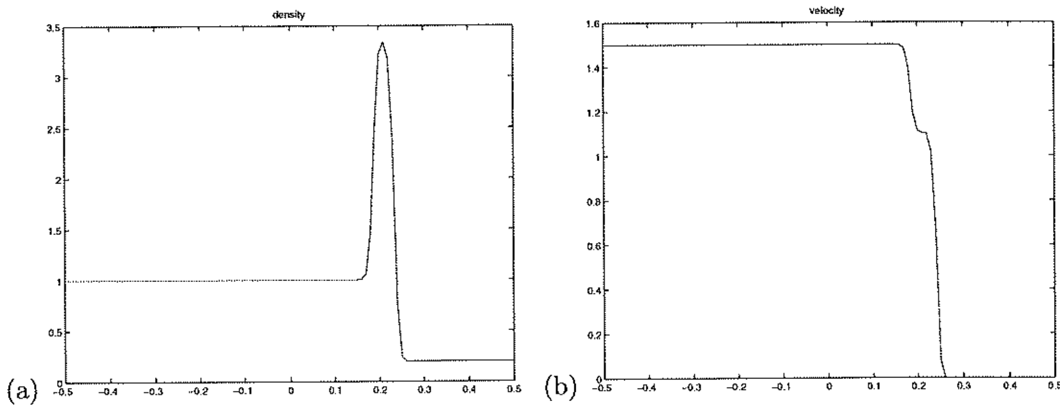

FIGURE 5.4. Density and velocity for $\epsilon = 0.07$

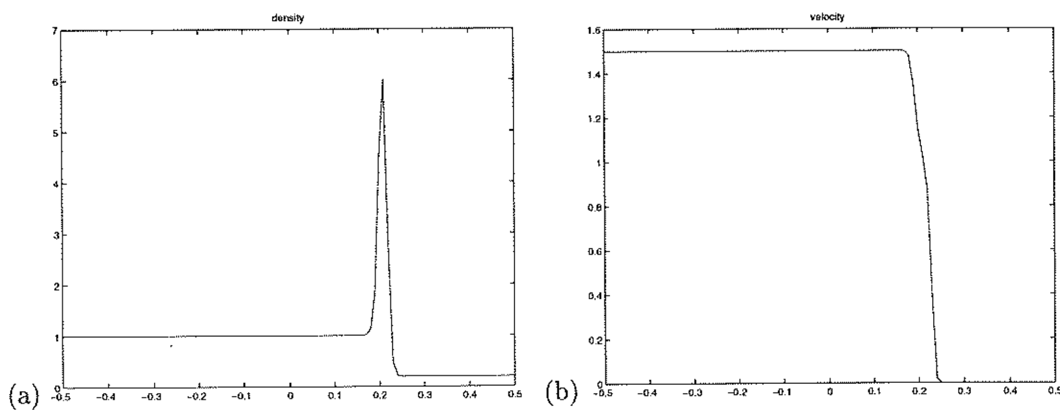

FIGURE 5.5. Density and velocity for $\epsilon = 0.014$

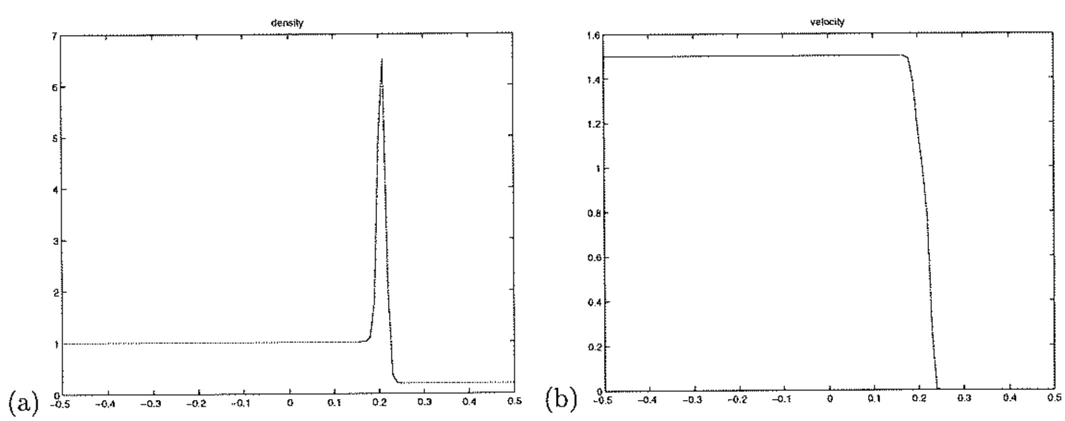

FIGURE 5.6. Density and velocity for $\epsilon = 0.0014$

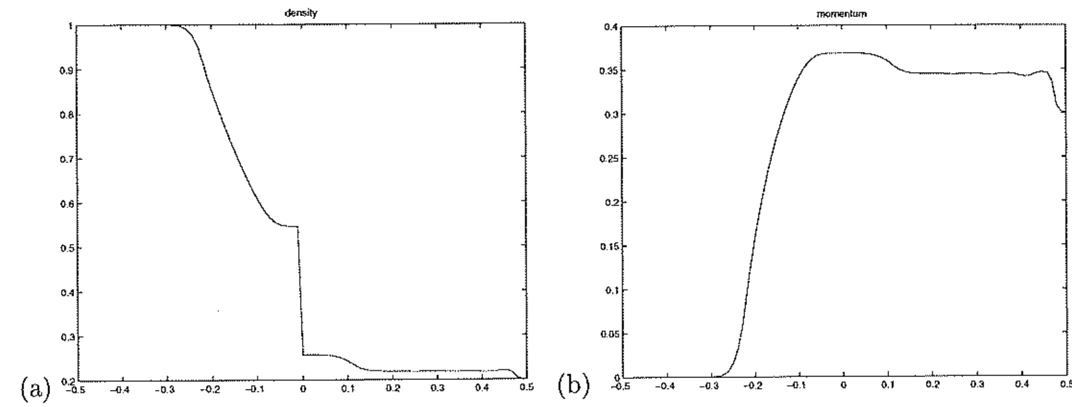

FIGURE 5.7. Density and momentum for $\epsilon = 1.4$

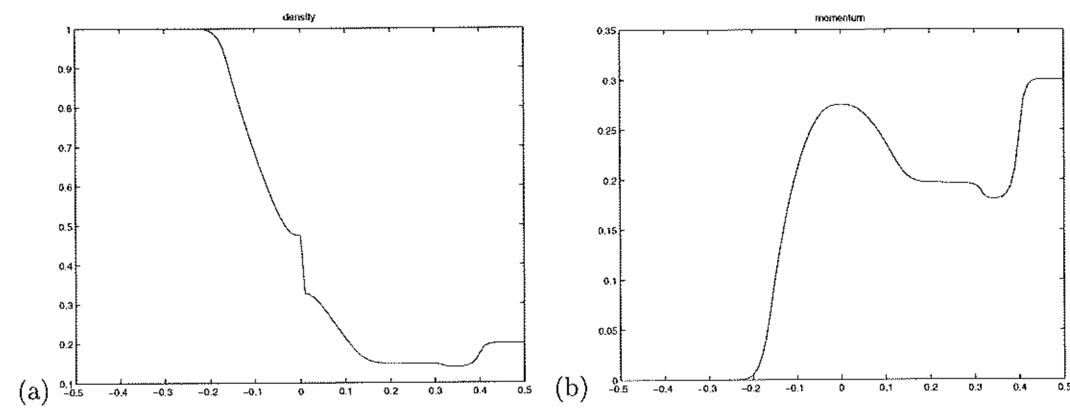

FIGURE 5.8. Density and momentum for $\epsilon = 0.7$

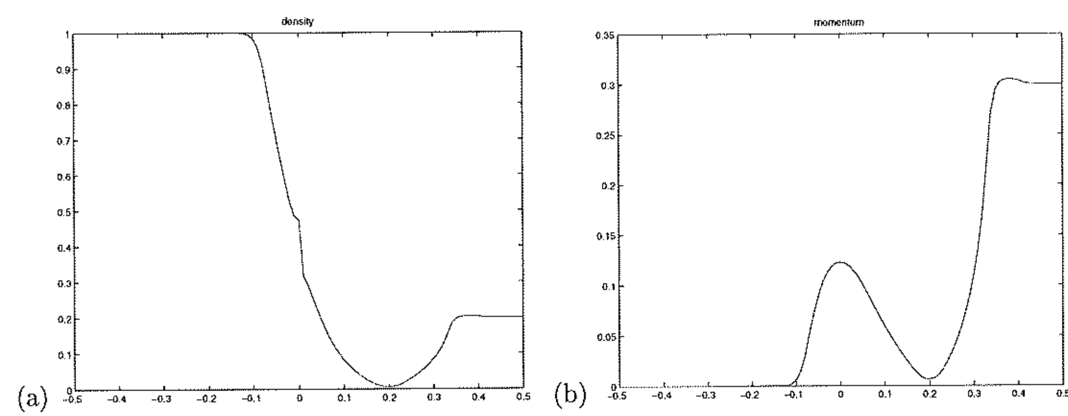

FIGURE 5.9. Density and momentum for $\epsilon = 0.14$

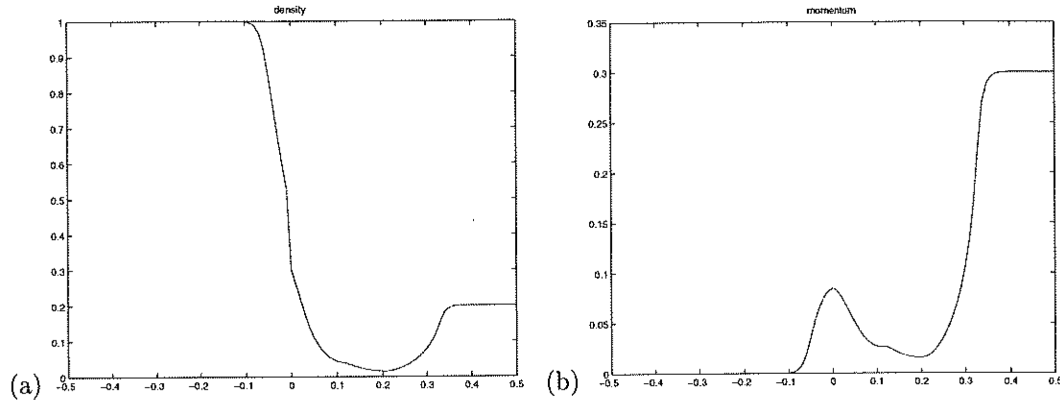

FIGURE 5.10. Density and momentum for $\epsilon = 0.07$

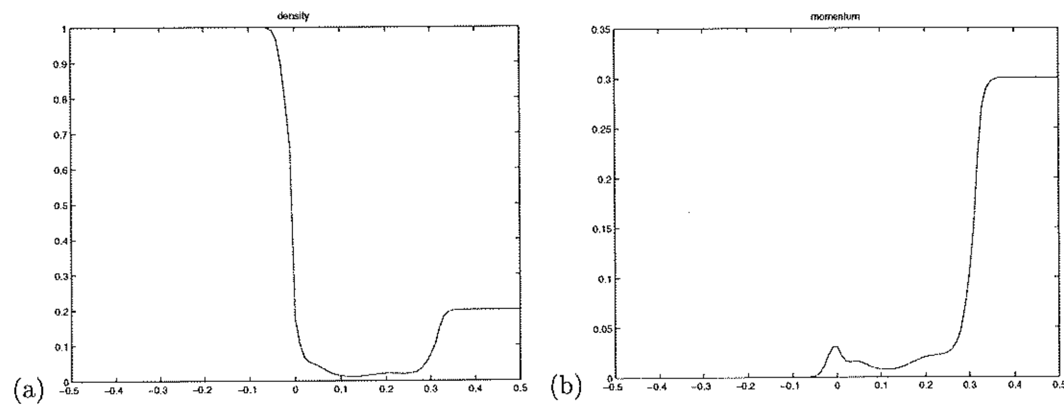

FIGURE 5.11. Density and momentum for $\epsilon = 0.014$

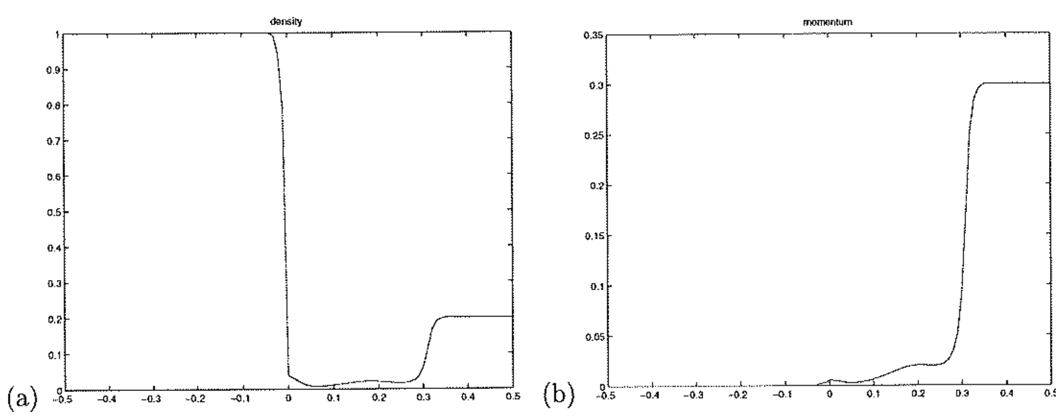

FIGURE 5.12. Density and momentum for $\epsilon = 0.0014$